Lithium Titanium Phosphate as Cathode, Anode and Electrolyte for Lithium Rechargeable Batteries

N. V. KOSOVA, D. I. OSINTSEV, N. F. UVAROV and E. T. DEVYATKINA

Institute of Solid State Chemistry and Mechanochemistry, Siberian Branch of the Russian Academy of Sciences, Ul. Kutateladze 18, Novosibirsk 630128 (Russia)

E-mail: kosova@solid.nsk.su

Abstract

Electrochemical properties and ionic conductivity of $LiTi_2(PO_4)_3$ (space group *R*-3*c*) synthesized using mechanical activation (MA) are investigated. It is established that MA decreases synthesis temperature and time allowing one to obtain the products of more homogeneous phase composition. The cycling ability of the samples is investigated with the help of a galvanostatic set-up in the electrochemical cell $LiTi_2(PO_4)_3$ (C)/($LiPF_6$ + EK + DMK/Li. It is established that within the potential range 2.0–3.5 V the capacity of the samples obtained with the help of MA is higher than that of the ceramic samples by about 20 %. Reversible cycling ability of $LiTi_2(PO_4)_3$, $NaTi_2(PO_4)_3$ and $KTi_2(PO_4)_3$ within the range 0.2–1.5 V was discovered. It may be due changes in the chemical composition of the electrode as a result of irreversible redox processes participated by PO_4 groups. It is shown that the conductivity of $LiTi_2(PO_4)_3$ and $Li_{1.3}Al_{0.3}Ti_{1.7}(PO_4)_3$ obtained using MA is 2–3 orders of magnitude higher than the conductivity of ceramic samples due to a decrease in resistance of the grain boundaries.

INTRODUCTION

During the recent years, subsequent to the pioneer works of Padhi [1], the development of a new generation of the cathode materials for lithium rechargeable batteries started on the basis of the use of phosphates of 3*d* metals with the frame structure able to intercalate/extract lithium ions reversibly. These materials differ from the corresponding oxides by relatively high lithium ion conductivity and increased working voltage, which is caused by the inductive effect of phosphate groups which decreases the covalence of Me–O bond thus decreasing the potential of Me^n/Me^{n-1} pair with respect to Li^+/Li^0. Much attention is paid to rather cheap and non-toxic iron phosphates with olivine ($LiFePO_4$) and nasicone $Li_3Fe_2(PO_4)_3$ structures having high discharge potential (3.4 and 2.8 V, respectively).

Rhombohedral $LiTi_2(PO_4)_3$ (space group *R*-3*c*) can intercalate up to two lithium ions reversibly, which is accompanied by the oxidation-reduction process Ti^{4+}/Ti^{3+}:

$$LiTi_2(PO_4)_3 + 2Li^+ + 2e^- \Leftrightarrow Li_3Ti_2(PO_4)_3$$

The working voltage for $LiTi_2(PO_4)_3$ is 2.48 V in comparison with 2.8 V for $Li_3Fe_2(PO_4)_3$; however, theoretical permittivity of the former is higher because titanium possesses smaller atomic mass that iron: 138 instead of 128 mA h/g. The first information about the cathode properties of $Li(Na)_{1+x}Ti_2(PO_4)_3$ was published in [2]. However, due to the low electronic conductivity, actual capacity of these compounds turned out to be substantially lower than the theoretical one; these compounds were considered to be unsuitable for use as cathode materials. A method of depositing a strong carbon coating as an electron-conducting additive onto the particle surface has been developed during the recent years; this measure solved the mentioned problem and allowed one to use $LiTi_2(PO_4)_3$ at high current density. According to the data obtained by authors [3], almost full theoretical capacity with relatively low polarization can be achieved during discharge of mechanochemically prepared composites of $LiTi_2(PO_4)_3$ with carbon.

The framework of $LiTi_2(PO_4)_3$ structure is formed by vertex-connected PO_4 tetrahedrons and TiO_6 jctahedrons [4]. Each PO_4 tetrahedron is connected with four TiO_6 octahedrons, and each TiO_6 octahedron is connected with six PO_4 tetrahedrons forming fragments (so-called lanterns) along the *c* axis. Lithium ions are distributed over positions M_1 (6*b*) and M_2 (18*e*); however, preferable positions are M_1 which are surrounded by six oxygen atoms and are situated in inversion centre. Temperature rise activates the movement between positions M_1 and M_2 coordinated by eight oxygen atoms. It was considered previously that additional lithium gets inserted into positions M_2, while positions M_1 are cleared gradually. However, it has been recently established by means of NMR that the formed $Li_3Ti_2(PO_4)_3$ belongs to space group *R*-3; lithium ions occupy two similar tetrahedral positions $M_{3'}$ and $M_{3''}$ at a ratio of 2/3 : 1/3 [5].

Lithium titanophosphate possesses relatively high ionic conductivity; its value is essentially dependent on impurities and on preparation method. This allows us to consider this compound not only as a cathode material but also as a promising electrolyte for inorganic solid-phase lithium rechargeable batteries. According to the data of [6–13], $LiTi_2(PO_4)_3$ obtained using the conventional ceramic procedure possesses ionic conductivity equal to $(2–3)\ 10^{-3}$ S/cm at 298 °C; however, the direct-current conductivity, determined by the resistance at grain boundaries, is only ~10^{-8}–10^{-7} S/cm due to high porosity and poor sintering quality of the ceramics. The use of low-melting and vitreous additives promoting sintering, as well as special methods of synthesis (*e.g.* spark plasma) allows one to increase this value to 10^{-6}–10^{-5} S/cm. The effective activation energy of conductivity is 0.3–0.4 eV. The authors of [7, 8] were the first to show that partial substitution of Ti^{4+} for Al^{3+} causes the most substantial (by almost 3 orders of magnitude) increase in the ionic conductivity of $Li_{1.3}Al_{0.3}Ti_{1.7}(PO_4)_3$ in comparison with non-doped $LiTi_2(PO_4)_3$. The synthesis was carried out by means of multiple heating of the mixture for tens hours with intermediate trituration. In spite of an increase in the concentration of labile carriers (lithium ions) as a result of $Ti^{4+} \leftrightarrow Al^{3+} + Li^+$ substitution and the possibility to perform transfer with the participation of these ions according to another mechanism (due to the higher occupation of eight-coordinated Li positions), the bulk conductivity did not change. An increase in conductivity was due to a decrease in the intergrain resistance as a result of an increase in the density of doped tablets during sintering. It was shown that conductivity is also affected by the impurity phases (TiO_2, TiP_2O_7 and $AlPO_4$) formed as a result of partial transition of lithium into the gas phase during synthesis and sintering.

It is known that preliminary mechanical activation (MA) of a mixture of reagents promoted a decrease in the synthesis temperature increasing the dispersity of the synthesized compounds and the homogeneity of their phase composition. It was shown in [14, 15] that mechanochemically obtained cathode materials possess improved electrochemical characteristics in some cases. The goal of the present work was to investigate the effect of MA at the stage of synthesis on conductivity and cycling ability of $LiTi_2(PO_4)_3$ and $Li_{1.3}Al_{0.3}Ti_{1.7}(PO_4)_3$.

EXPERIMENTAL

Lithium titanophosphate was obtained by means of solid-phase synthesis from the activated and non-activated mixtures of initial reagents: TiO_2, Li_2CO_3 and $NH_4H_2PO_4$ of "ch.d.a." reagent grade. The initial mixture taken in the stoichiometric ratio was preliminarily heated at 400 °C to remove ammonia and water, then the mixture was activated for 5 min in the air with EI-2×150 centrifugal planetary mill with the cylinders and balls made of titanium. The activated and non-activated mixtures were annealed at 800–1000 °C for 4 h. In order to synthesize Al-substituted $LiTi_2(PO_4)_3$, a stoichiometric amount of gibbsite $Al(OH)_3$ was introduced into the initial mixture. In order to meet the electroneutrality requirement, total lithium content was increased till the composition of $Li_{1.3}Al_{0.3}Ti_{1.7}(PO_4)_3$.

The samples were investigated by means of X-ray phase analysis (XPA), infrared spectroscopy (IRS), complex impedance and chronopotentiometry. Powder diffraction

patterns were recorded with DRON-3.0 diffractometer (CuK_α radiation), IR spectra were recorded with FTIR Specord-75 spectrometer of Bruker company within the range 200–4000 cm^{-1}. Conductivity of the samples was measured with alternating current with the help of impedance-measuring device HP-4284A within the frequency range $20–10^{-6}$ Hz using tablets with silver electrodes. Before measurements, the tablets pressed at ~0.7 GPa were agglomerated at a temperature corresponding to the synthesis temperature. The cycling ability of samples was studied with a galvanostatic set-up in $LiTi_2(PO_4)_3/LiPF_6$ + EK + DMK/Li electrochemical cell with the charging/discharging rate S/20. In order to increase the electronic conductivity, acetylene black was added to the cathode material in the amount of 20 %.

RESULTS AND DISCUSSION

The sub-solidus diagram of state for the $Li_2O–TiO_2–P_2O_5$ system is shown in Fig. 1. The formation of two ternary compounds is possible in this system: $LiTi_2(PO_4)_3$ and $LiTiPO_5$. According to the data of [6–13], both pure and doped $LiTi_2(PO_4)_3$ is formed after long-term multistage heating of a mixture of the corresponding reagents. The final temperature of formation is 900–1000 °C. With an increase in temperature and duration of synthesis, on the one hand, the degree of interaction of the initial reagents increases; on the other hand,

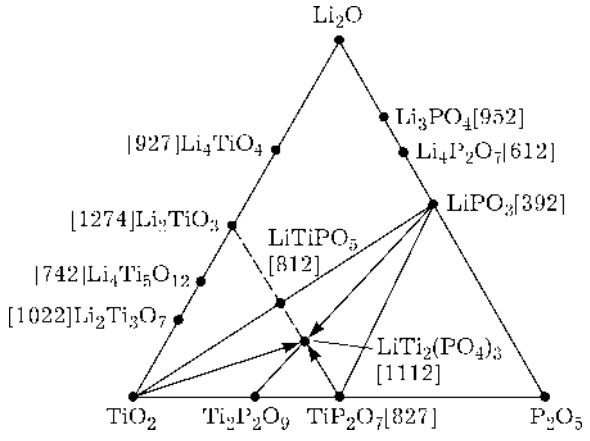

Fig. 1. Sub-solidus diagram of states of the $Li_2O–TiO_2–P_2O_5$ system. Melting points, °C, are shown in square brackets.

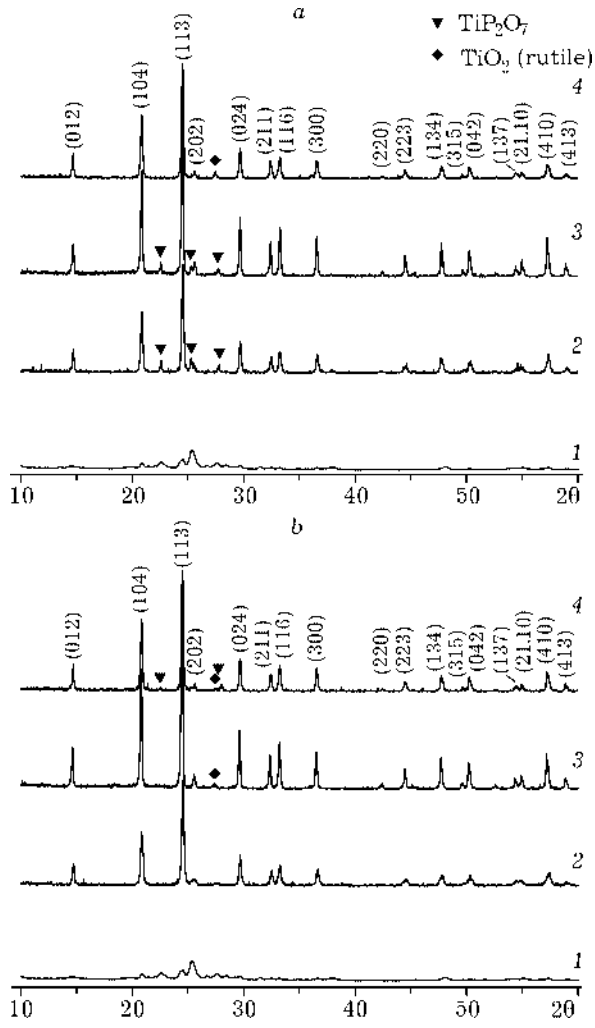

Fig. 2. X-ray diffraction patterns of $LiTi_2(PO_4)_3$ obtained by heating the non-activated (*a*) and activated (*b*) reagent mixtures up to temperature, °C: 400 (*1*), 800 (*2*), 900 (*3*), 1000 (*4*); *1* – TiP_2O_7, *2* – TiO_2 (rutile); indices relate to $LiTi_2(PO_4)_3$.

thermal decomposition of $LiTi_2(PO_4)_3$ occurs as a result of partial transition of Li_2O into the gas phase (for $T > 800$ °C):

$$2LiTi_2(PO_4)_3 \rightarrow Li_2O\uparrow + TiO_2 + 3TiP_2O_7$$

Investigations showed that the synthesis of $LiTi_2(PO_4)_3$ in preliminarily activated mixtures is completed at lower (below 800 °C) temperature in comparison with non-activated ones, and results in the formation of a product more homogeneous in phase composition at the given temperature (Fig. 2). Non-doped products obtained from non-activated mixtures contain TiP_2O_7 and rutile as extrinsic phases, while the Al-substituted sample contains $AlPO_4$.

The unit cell parameters of $LiTi_2(PO_4)_3$ and $Li_{1.3}Al_{0.3}Ti_{1.7}(PO_4)_3$ samples synthesized at

TABLE 1

The calculated lattice parameters for the samples

T_{syn}, °C	Initial		Mechanically activated	
	$a \pm \Delta a$, nm	$c \pm \Delta c$, nm	$a \pm \Delta a$, nm	$c \pm \Delta c$, nm
		$LiTi_2(PO_4)_3$		
800	0.8496 ± 0.0006	2.087 ± 0.004	0.8502 ± 0.0004	2.095 ± 0.003
900	0.8513 ± 0.0001	2.085 ± 0.001	0.8512 ± 0.0002	2.085 ± 0.001
1000	0.8501 ± 0.0003	2.086 ± 0.002	0.8499 ± 0.0003	2.082 ± 0.002
		$Li_{1.3}Al_{0.3}Ti_{1.7}(PO_4)_3$		
800	0.8490 ± 0.0004	2.085 ± 0.003	0.8485 ± 0.0005	2.085 ± 0.004
900	0.8505 ± 0.0003	2.084 ± 0.002	0.8492 ± 0.0003	2.079 ± 0.002
1000	0.8499 ± 0.0004	2.083 ± 0.003	0.8499 ± 0.0003	2.082 ± 0.002

different temperature T_{syn} from activated and non-activated mixtures are shown in Table 1. According to the data published in [9, 13], the a and c parameters for $LiTi_2(PO_4)_3$ are 0.85129 and 2.0878 nm, respectively; for $Li_{1.3}Al_{0.3}Ti_{1.7}(PO_4)_3$ the corresponding parameters are 0.850 and 2.082 nm, respectively. The introduction of Al causes only insignificant decrease in these parameters, which correlates with the ion radii: $R_{Al^{3+}}$ = 0.0535 nm, $R_{Ti^{4+}}$ = 0.0605 nm. It follows from the data presented in Table 1 that MA has no substantial effect on the cell parameters for $LiTi_2(PO_4)_3$ and $Li_{1.3}Al_{0.3}Ti_{1.7}(PO_4)_3$. The unit cell parameters for the samples obtained at 900 °C are the closest to the literature data.

The IR spectra of the samples of pure and Al-substituted $LiTi_2(PO_4)_3$ obtained after heating the activated and non-activated mixtures at a temperature of 900 °C are shown in Fig. 3. Four groups of vibrations can be distinguished in all the spectra observed: within the regions 270–300, 300–550, 550–700 and 800–1200 cm^{-1}. The major contribution into the intensity of IR bands is made by the vibrations of PO_4 groups. According to the factor group analysis, the isolated PO_4^{3-} anion with the point symmetry group T_d has 4 modes: one A_1 {ν_1; $\nu_s(PO_4)$}, one E {ν_2; $\delta_s(PO_4)$} and two F_2 ({$\nu_{3,4}$; $\nu_{as}(PO_4)$ and $\delta_{as}(PO_4)$}). All the modes are allowed in the Raman spectra but only ν_3 and ν_4 are allowed in the IR. The authors of [16] who investigated $Mn_{0.5+x}Ti_{2-2x}Cr_{2x}(PO_4)_3$ with space group R-3c observed the IR vibrations of PO_4 groups in the regions 370–400, 550–650 and 900–1150 cm^{-1}. Similar vibrations of PO_4 groups were also observed by the authors of [17] when investigating ammonium zirconophosphates with nasicone structure. The intensity of absorption bands in the regions 320–550 and 550–650 cm^{-1} is also contributed by the stretching vibrations of TiO_6 groups.

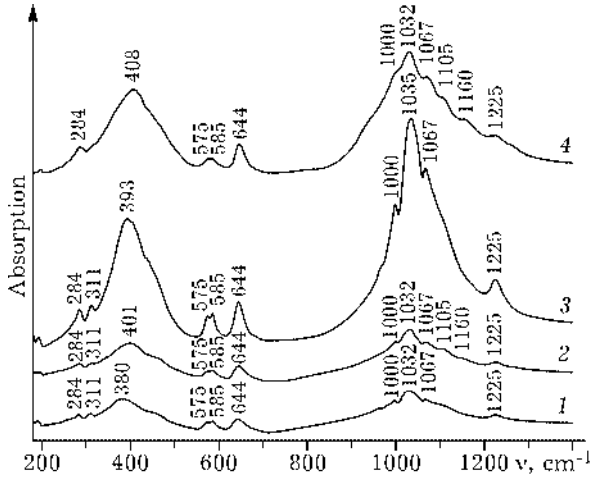

Fig. 3. IR spectra of $LiTi_2(PO_4)_3$ (*1*, *3*) and $Li_{1.3}Al_{0.3}Ti_{1.7}(PO_4)_3$ (*2*, *4*) recorded for non-activated (*1*, *2*) and activated (*3*, *4*) mixtures. T_{syn} = 900 °C.

With the substitution of a part of Ti^{4+} for Al^{3+}, the positions of all the bands mentioned above remain almost unchanged; however, broadening of vibration bands in the regions 300–550 and 800–1200 cm^{-1} is observed. The high-frequency bands in the spectra of $Li_{1.3}Al_{0.3}Ti_{1.7}(PO_4)_3$ have a more complicated shape, which is an evidence of some distortion or non-equivalency of vibrations of different PO_4^{3-} groups due to the insertion of Al^{3+} ions into the structure. This is confirmed by the data of ^{31}P NMR spectroscopy [9] suggesting that a narrow band at −28 ppm, which is

characteristic of orthophosphates, becomes wider and asymmetric after partial substitution of titanium for aluminium.

In spite of the absence of substantial differences in the spectra of samples prepared using MA and without it, attention should be paid to the fact that the intensity of vibration bands in the activated samples is much higher.

The results of investigation of ionic conductivity of the samples synthesized at 800, 900 and 1000 °C are shown in Figs. 4, 5 and in Table 2. One can see that for any synthesis temperature the conductivity of samples obtained with the help of MA is substantially (by 2–3 orders of magnitude) higher than that of the ceramic samples[1], while the activation energy of conductivity is lower[2]. The conductivity of aluminium-substituted samples is 1–2 orders of magnitude higher than that of non-substituted samples. The maximal conductivity is observed for the samples synthesized at 900 °C, for which we succeeded to distinguish the contributions from the bulk conductivity (σ_{hf}) and the resistance of grain boundaries (σ_{dc}). It turned out that the bulk conductivity of the samples obtained using MA remains almost unchanged or even slightly decreases in the case on non-doped $LiTi_2(PO_4)_3$. Substitution has only slight effect and MA has almost no effect on the activation energy of bulk conductivity. An increase in the ionic conductivity of the samples occurs only due to a decrease in the resistance of grain boundaries.

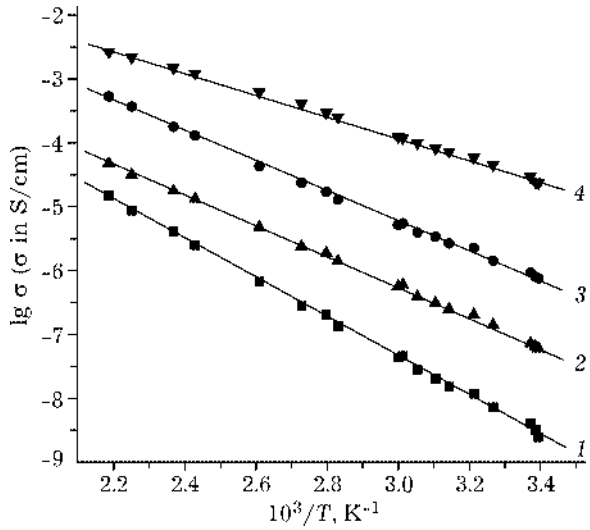

Fig. 4. Arrhenius dependencies of the direct-current conductivity within temperature range 20–200 °C for $LiTi_2(PO_4)_3$ (*1, 3*) and $Li_{1.3}Al_{0.3}Ti_{1.7}(PO_4)_3$ (*2, 4*) samples obtained from non-activated (*1, 2*) and activated (*3, 4*) mixtures. T_{syn} = 800 °C.

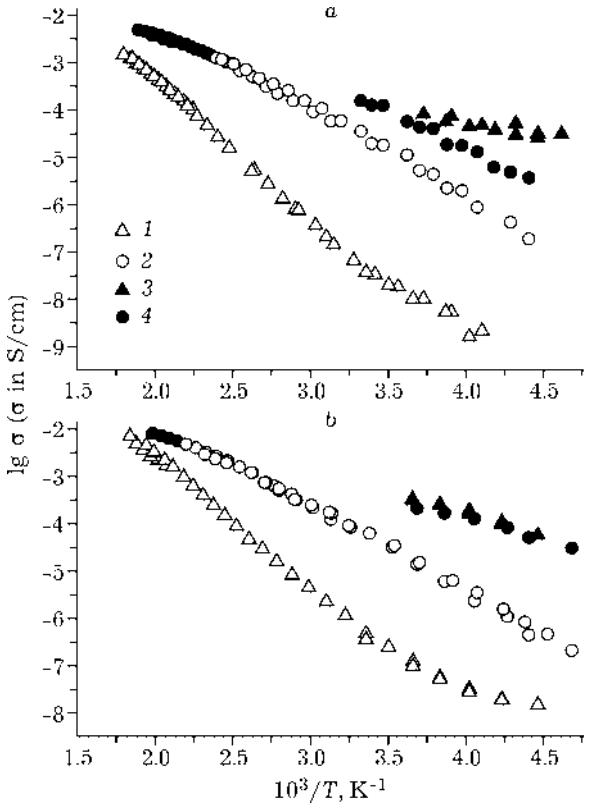

Fig. 5. Arrhenius dependencies of conductivity within temperature range −60...+300 °C for $LiTi_2(PO_4)_3$ (*a*) and $Li_{1.3}Al_{0.3}Ti_{1.7}(PO_4)_3$ (*b*) samples obtained from non-activated (*1, 3*) and activated (*2, 4*) mixtures (T_{syn} = 900 °C): *1, 2* – direct-current conductivity due to the resistnace of boundaries between grains; *3, 4* – bulk conductivity.

[1] For the samples synthesized within the present work by means of the ceramic procedure, the observed conductivity turned out to be lower than that described in literature, which is connected with substantial decrease in sintering time (single heating for 4 h instead of multiple heatings for tens hours).

[2] In order to calculate the activation energy E_a of conductivity, at first the parameters of the equivalent scheme taking into account sequential connection of the grain boundaries R_{gb} and the bulk material $R_b = 1/s \cdot L/s$ (where L and s are thickness and area of the electrode, respectively) were determined with the help of the analysis of impedance hodographs. Temperature dependencies of the resistance of grain boundaries and of the bulk conductivity were described by the Arrhenius curves, so E_a values were determined by minimizing the square mean deviation of the calculated data from the experimental values for the conductivity within a broad temperature range. The accuracy of determination of E_a was ±0.02 eV for the resistance of grain bodunaries and ±0.03 eV for the bulk conductivity.

TABLE 2

Ionic conductivity and activation energy for the synthesized samples

Sample	T_{syn}, °C	MA	σ_{dc} (25 °C), S/cm	$E_{a\,dc}$, eV	σ_{hf} (25 °C), S/cm	$E_{a\,hf}$, eV
$LiTi_2(PO_4)_3$	800	−	$3.2 \cdot 10^{-9}$	0.64 (20−185 °C)	−	−
		+	$8.1 \cdot 10^{-7}$	0.50 (20−185 °C)	−	−
	900	−	$3.6 \cdot 10^{-8}$	0.68 (25−180 °C)	$1.1 \cdot 10^{-4}$*	0.20 (−55...0 °C)
		+	$2.0 \cdot 10^{-5}$	0.44 (−45...+145 °C)	$1.3 \cdot 10^{-4}$	0.27 (−45...+30 °C)
	1000	−	$1.9 \cdot 10^{-8}$	0.58 (0−225 °C)	−	−
		+	$5.1 \cdot 10^{-7}$	0.49 (−45...+225 °C)	$2.5 \cdot 10^{-5}$	0.30 (−55...+40 °C)
$Li_{1.3}Al_{0.3}Ti_{1.7}(PO_4)_3$	800	−	$6.0 \cdot 10^{-8}$	0.49 (20−185 °C)	−	−
		+	$2.4 \cdot 10^{-5}$	0.36 (20−185 °C)	−	−
	900	−	$3.4 \cdot 10^{-7}$	0.61 (20−185 °C)	$6.3 \cdot 10^{-4}$*	0.23 (−50...0 °C)
		+	$6.2 \cdot 10^{-5}$	0.40 (−60...+180 °C)	$4.6 \cdot 10^{-4}$*	0.22 (−60...0 °C)
	1000	−	$1.4 \cdot 10^{-6}$	0.57 (−5...+170 °C)	$4.5 \cdot 10^{-4}$	0.14 (−20...+100 °C)
		+	$2.0 \cdot 10^{-7}$	0.75 (60−170 °C)	$4.6 \cdot 10^{-4}$	0.13 (−20...+100 °C)
				0.13 (−20...+30 °C)		

*The data were obtained by extrapolation.

In our opinion, this may be due to several reasons, including a decrease in the concentration of dielectric impurities in the surface layer (which is confirmed by the XPA data); an increase in the number of contacts between the particles due to better agglomeration of the particles obtained using MA; an increase in concentration and acceleration of the diffusion of lithium ions in the sub-surface layer due to an increase in vacancy disordering (which was observed for fine lithium conductors [19]. This question requires further investigation. It should be noted that the pycnometric density of the samples prepared using MA turned out to be somewhat lower than for the ceramic samples, which is an indirect evidence of the presence of internal pores which nevertheless prevent the transport of lithium ions.

A deviation of the experimental Arrhenius dependence from the straight line (see Fig. 5) is caused by the fact that at high temperature the resistance of grain boundaries is comparable with the bulk resistance of the sample. Within the low-temperature region, a decrease in the activation energy is likely to be explained by the presence of impurities on grain boundaries which simplify transport of lithium ions through the inter-phase contact.

So, MA helped to achieve the direct-current conductivity at room temperature for $LiTi_2(PO_4)_3$ and $Li_{1.3}Al_{0.3}Ti_{1.7}(PO_4)_3$ equal to $2.0\,10^{-5}$ and $6.2\,10^{-5}$ S/cm, respectively. It is interesting that MA to a larger extent promotes an increase in the conductivity of non-doped $LiTi_2(PO_4)_3$. Such a high value for $LiTi_2(PO_4)_3$ was obtained by the authors of [10] using the spark plasma method

The first discharge curves for $LiTi_2(PO_4)_3$ within the range 3.5−2.0 V are shown in Fig. 6. The discharge voltage was ~2.47 V both for the activated and for non-activated samples, which correlates with the literature data [3]. The plateau points to the two-phase mechanism of lithium ion insertion and is due to the formation of a new phase $Li_3Ti_2(PO_4)_3$. The actual specific permittivity of the sample obtained without using MA turned out to be equal to 87 mA h/g at the first cycle. The use of MA in the synthesis caused an increase in this value by ~20 % (105 mA h/g), which, in our opinion, is connected with a decrease in particle size and thus with a more complete involvement of the volume of the active cathode material.

Comparative investigation of the cycling ability of $LiTi_2(PO_4)_3$, $NaTi_2(PO_4)_3$ and $KTi_2(PO_4)_3$ showed that lithium phosphate is characterized by the highest capacity. For $NaTi_2(PO_4)_3$, the discharge plateau was observed for lower potential (~2.4 V) than that for $LiTi_2(PO_4)_3$, while permittivity at the first cycle was 70 mA h/g. For $KTi_2(PO_4)_3$, a smooth

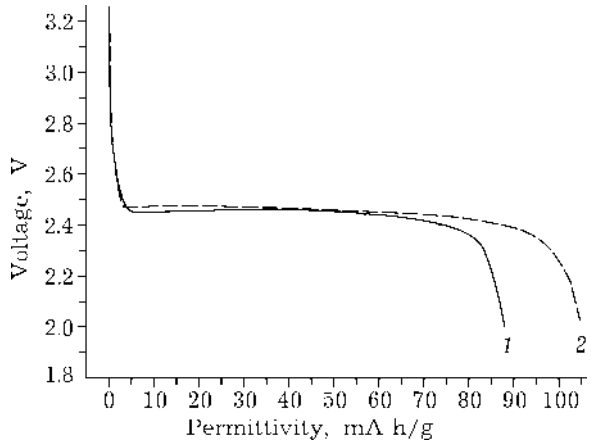

Fig. 6. First discharge curves for $LiTi_2(PO_4)_3$ obtained form non-activated (*1*) and activated (*2*) mixtures within the range 2.0–3.5 V (j ~ 0.1 mA/cm^2).

decrease in voltage was observed in the discharge curve instead of a plateau, which, as a rule, points to the formation of solid solutions resulting from lithium ion insertion.

Deep discharge (to 0.2 V) for $MeTi_2(PO_4)_3$ (Me = Li, Na, K) revealed the possibility to insert more than two additional lithium ions into the cathode material, which cannot be explained only by the reduction of Ti^{4+} to Ti^{3+}. At the first cycle, the discharge capacity for all the samples was >250 mA h/g, which is more than 2 times as large as the theoretical value. For the Li sample, a gently sloping region was observed for 0.7–0.9 V at the discharge curve. For all the $MeTi_2(PO_4)_3$ samples, reversibility of lithium ion insertion-extraction was observed within the low-voltage region 0.2–1.5 V (Fig. 7), which is characteristic of anode materials. At the same time, substantial worsening of the next cycling steps in the high-voltage region (above 1.5 V) was observed, which is an evidence of irreversible changes occurring with the cathode material.

In the opinion of the authors of [19], who were the first to investigate cycling of $LiTi_2(PO_4)_3$ in the anode region, insertion of additional lithium ions occurs due to the participation of PO_4 groups in redistribution of the electronic density over the inter-phase surface of $LiTi_2(PO_4)_3$ particles contacting with the electrolyte, In our opinion, this phenomenon can be explained by changes in the chemical composition of the surface of electrode particles as a result of irreversible redox processes

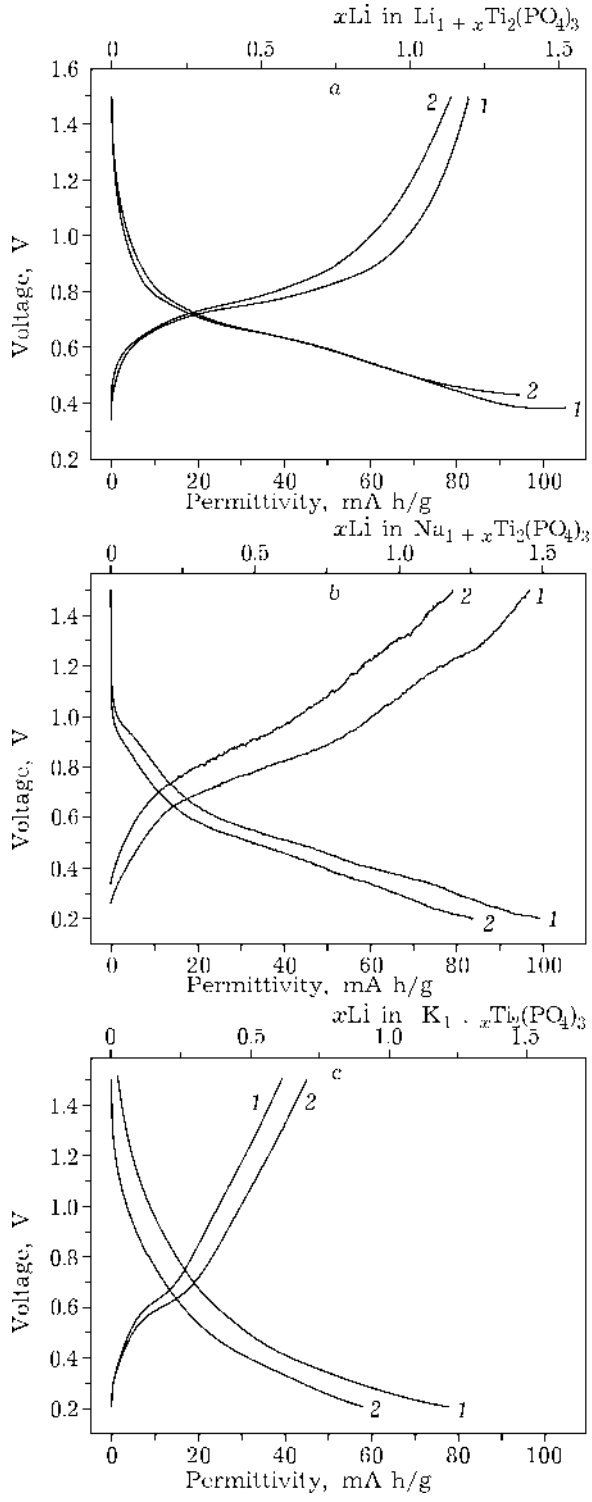

Fig. 7. Discharge-charge curves for $MeTi_2(PO_4)_3$ within the range 0.2–1.5 V (j ~0.1 mA/cm^2). Me = Li (*a*), Na (*b*), K (*c*); *1*, *2* – numbers of charge/discharge events.

participated by PO_4 groups. The formation of titanium phosphides may occur (for example, Li_7TiP_4); these compounds possess the ability to reversible cycling within the range 0.2–1.5 V [20].

CONCLUSION

So, it is established that the use of MA at the stage of synthesis causes substantial improvement of the ionic conductivity and an increase in the specific capacity of $LiTi_2(PO_4)_3$ and $Li_{1.3}Al_{0.3}Ti_{1.7}(PO_4)_3$, which opens the outlooks to use the materials, obtained with the help of the above-described procedure, as a cathode, anode and a solid crystal electrolyte for lithium rechargeable batteries.

REFERENCES

1 A. K. Padhi, K. S. Nanjundaswamy, J. B. Goodenough, *J. Electrochem. Soc.*, 144 (1997) 1188.
2 C. Delmas, A. Nadiri, J. L. Soubeyroux, *Solid State Ionics*, 28–30 (1988) 419.
3 S. Patoux, C. Masquelier, Meeting Abstracts of 11 Int. Meeting on Lithium Batteries, Monterey, CA, June 23–28, 2002.
4 A. G. Belous, G. N. Novitskaya, S. V. Polyanitskaya, Yu. I. Gornikov, *Izv. AN SSSR. Neorg. Mat.*, 23 (1987) 470.
5 A. Aatiq, M. Menetrier, L. Croguennec *et al.*, *J. Mater. Chem.*, 12 (2002) 2971.
6 H. Aono, E. Sugimoto, Y. Sadaoka *et al.*, *J. Electrochem. Soc.*, 137 (1990) 1023.
7 H. Aono, E. Sugimoto, Y. Sadaoka *et al.*, *Ibid.*, 136 (1989) 590.
8 H. Aono, E. Sugimoto, Y. Sadaoka *et al.*, *Chem. Lett.*, 1990 (1990) 1825.
9 S. Wong, P. G. J. Newman, A. S. Best *et al.*, *J. Mat. Chem.*, 8(10) (1998) 2199.
10 Y. Kobayashi, T. Takeuchi, M. Tabuchi *et al.*, *J. Power Sources*, 81–82 (1999) 853.
11 Y. Kobayashi, M. Tabuchi, O. Nakamura, *Ibid.*, 68 (1997) 407.
12 K. Takada, M. Tansho, I. Yanase *et al.*, *Solid State Ionics*, 139 (2001) 241.
13 A. S. Best, M. Forsyth, D. R. MacFarlane, *Ibid.*, 136–137 (2000) 339.
14 N. V. Kosova, E. T. Devyatkina, V. F. Anufrienko *et al.*, *Chem. Sustain. Develop.*, 10 (2002) 81. http://www-psb.ad-sbras.nsc.ru
15 N. Kosova, E. Devyatkina, *Ann. Chem. Sci. Mater.*, 27 (2002) 77.
16 R. Pikl, D. de Waal, A. Aatiq, A. El Jazouli, *Vibrational Spectroscopy*, 16 (1998) 137.
17 M. V. Chaikina, V. A. Sadykov, S. N. Pavlova *et al.*, *J. Mat. Synth. Proc.*, 8, 5–6 (2000) 279.
18 P. Heitjans, S. Indris, *J. Phys.: Condens. Matter*, 15 (2003) R1257.
19 G. X. Wang, D. H. Bradhurst, S. X. Dou, H. K. Liu, *J. Power Sources*, 124 (2003) 231.
20 L. Monconduit, F. Gillot, M.–L. Doublet *et al.*, Meeting Abstracts of 11 Int. Meeting on Lithium Batteries, Monterey, CA, June 23–28, 2002.